Proof

Gorgan University of Agricultural Sciences and Natural Resources

Environmental Resources Research (ERR)

Print ISSN: 2783-4832
Online ISSN: 2783-4670

Analysis of Temperature and Precipitation Parameters using the General Atmospheric Circulation Model, Sixth Report (Case Study: Aleshtar Synoptic Station)

Article Info

Article type:
Research Article

Article history:
Received:
Accepted:

Corresponding author:

Keywords:
Climate Change
Aleshtar
Simulation
General Circulation Model

Abstract

Regional assessments of climate change are critical for understanding future challenges. This study assesses the impact of climate change on the Aleshtar Synoptic Station (Lorestan Province, Iran) by applying the CanESM5.0 climate model (CMIP6) to project future temperature and precipitation under SSP1-2.6, SSP2-4.5, and SSP5-8.5 scenarios for 2031–2050 and 2051–2070. Downscaling was performed using LSRS-WG. Key findings include: under SSP1-2.6, decreasing trends in minimum temperature and precipitation; increased maximum temperature; increasing temperature trends from June–October; and increased precipitation from January–June and October–December. Seasonal analyses showed rising temperature in spring and summer, and increasing precipitation in autumn and winter. This research offers valuable insights for water resource management, climate adaptation planning, and informed policy

Cite this article: ----------. 2026. Analysis of Temperature and Precipitation Parameters using the General Atmospheric Circulation Model, Sixth Report (Case Study: Aleshtar Synoptic Station): A Case Study of Iran. *Environmental Resources Research*, 14(1), 81-92.

Publisher: Gorgan University of Agricultural Sciences and Natural Resources

Introduction

Climate change has become a global threat that significantly impacts the water resources sector (Adhikari et al., 2015; Amirabadi-zadeh et al., 2016). In the past two decades, climate change has been one of the most important and controversial topics among climatologists. Humanity, as part of the climate system, significantly influences climate behavior. Today, with increasing population and, consequently, increasing demand for water and food, agricultural expansion, deforestation, desertification, and the growing use of fossil fuels, the human role in climate change has become more prominent than ever (Jahangir et al., 2022). In recent years, with the increasing global warming, the changes in abnormal events continue to grow larger. For instance, extreme heat waves that previously occurred once every decade now happen approximately three times in ten years. With merely half a degree Celsius increase in the global average temperature, such heat waves will occur four times per decade, and the resulting temperature will be nearly two degrees Celsius hotter. If global warming continues, the frequency and intensity of record-breaking rainfall events and droughts will similarly increase. The probability of severe droughts, which previously occurred approximately once every decade, has increased by 70%, and if the world warms by two degrees Celsius, this number could double (IPCC Sixth Assessment Report, 2021). Due to global warming, the trend of destructive droughts and floods has also increased (Weijing et al., 2015; Zhang, 2015; Si et al., 2016). To work with GCMs, downscaling methods, typically dynamic and statistical methods, are commonly used. These methods are employed to address the challenge of spatial development in GCMs. This is achieved by linking large-scale atmospheric variables with climatic parameters at a local scale. Downscaling methods convert the large-scale output of GCMs into high-resolution output for the studied region (Saref & Reggular, 2016; Gebrchorcus et al., 2019, Mwabumba et al., 2022). Ferreira et al. (2018) studied summer precipitation fluctuations in the southeastern United States and showed that with increasing air temperature and humidity, precipitation will increase in the future in that region. Jiang et al. (2020) evaluated precipitation changes in Central Asia until the end of the 21st century using data from 15 CMIP6 models under SSP scenarios. The results indicated an increasing trend in the average annual precipitation across all climatic scenarios in the study area. Heydari et al. (2020) studied precipitation and temperature fluctuations in the Urmia River basin using HadGEM2 model data and showed that precipitation would decrease and temperature would increase in the future. Keown et al. (2021) investigated the trend of precipitation and air temperature changes in Northwest China using data from 5 CMIP6 models and showed that CMIP6 models simulate air temperature better than precipitation. They also showed that precipitation and air temperature would increase under future scenarios in the study area. Javaherian et al. (2021) used the CanESM2 predictive model based on RCP scenarios (RCP2.6, RCP4.5, and RCP8.5) for the period 2020-2060 and the SDSM model for downscaling daily precipitation and temperature parameters over an 11-year base period (1984-1995) to predict the effects of climate change on the Lar Dam basin in Fars province. The results of this study indicated that daily average temperature would increase by 1.01 to 1.12 degrees Celsius, and daily precipitation would increase by 21 to 23 percent across all three studied scenarios. Qin et al. (2021) evaluated precipitation and air temperature fluctuations in Northwest China using CMIP6 models and showed that these models could simulate temperature better than precipitation. They also showed that average temperature and precipitation would significantly increase in various scenarios in the 21st century in the study area. Yu et al. (2021) studied average temperature fluctuations in China using 20 GCMs from CMIP6 models and three SSP scenarios, showing that average temperature would increase in future scenarios. Basil et al. (2022) investigated the effects of climate change on precipitation and air temperature parameters in the two provinces of Buenos Aires and Córdoba in Argentina and showed that annual maximum and average

temperatures would increase in both studied provinces. They also showed an upward trend in precipitation during autumn and winter. Trai et al. (2022) evaluated the performance of CMIP5 and CMIP6 models in simulating precipitation and discharge parameters in the Mekong River basin at the border between China, Myanmar, Thailand, Laos, Cambodia, and Vietnam, showing that CMIP6 models have higher accuracy compared to CMIP5 models. They also showed that, according to CMIP6 model results, effective precipitation and annual peak discharge would increase under SSP scenarios. Majdi et al. (2022) evaluated precipitation and temperature fluctuations in the Middle East and North Africa, showing that air temperature would increase by 0.8 to 3.3 degrees Celsius, and precipitation would decrease by 5 to 133 millimeters. Zhang et al. (2022) studied the temporal and spatial characteristics of convective and large-scale precipitation in Southeast China using MERRA-2 model data and showed that total precipitation and large-scale precipitation would increase in future periods. Acar and Gönçigil (2022) assessed the trend of precipitation changes at 142 synoptic stations in Turkey and showed that in most of the studied stations, the precipitation trend is upward in winter, and overall, precipitation in the study area will have a decreasing trend.

Based on the research conducted, it is clear that the selection of General Circulation Models (GCMs) is critical and important due to computational limitations and fundamental uncertainties. Furthermore, with the increase in global surface temperature, it is necessary to evaluate its regional impact for a more accurate understanding of future challenges and related planning. On the other hand, considering that the selseleh plain has faced a significant decrease in rainfall and increase in temperature in recent years, and also the production of crops in this plain has decreased, therefore, investigating the climatic conditions of the selseleh plain is a necessary and essential matter, which can greatly help in developing a plan for adaptation to water scarcity.Therefore, this research will examine the impact of climate change on temperature and precipitation parameters using CMIP6 climate models in the selseleh County of Lorestan Province, utilizing data from the CanESM5 prediction model and the LARS-WG downscaling model based on designed emission scenarios in the baseline period of 1997to 2022 to predict the atmospheric conditions during the future period. Three scenarios will be used for the twenty-year periods in the near future from 2031-2050 and 2051-2100 : the optimistic SSP126, the intermediate SSP245, and the pessimistic SSP585.

Materials and Methods

Study Area

Lorestan Province, located in Iran, is one of the mountainous regions in western Iran, predominantly covered by the Zagros Mountains. The climate of Lorestan Province is diverse, with noticeable variations from the northeast to the southwest. One of the most significant and water-rich plains in this province is the Selseleh (or Aleshtar) Plain. This plain is situated between longitudes 48° 2' to 48° 31' E and latitudes 33° 43' to 34° 05' N, with an average elevation of about 1,580 meters above sea level and an area of 196 km². The average annual rainfall in the plain is 54 mm, and the mean annual temperature is 8.8°C. Topographically, the plain consists of lowlands, relatively flat areas, mountains, and foothills. The mountains in the region, which play a significant role in the formation and development of alluvial systems, are largely influenced by two key factors: climate and tectonic movements. The fractures and faults in this area have created suitable channels for water flow, thus playing a crucial role in the formation of channeled streams. Figure 1 shows the geographical location of the study area. Precipitation and temperature graphs are displayed in Figures 2 and 3.

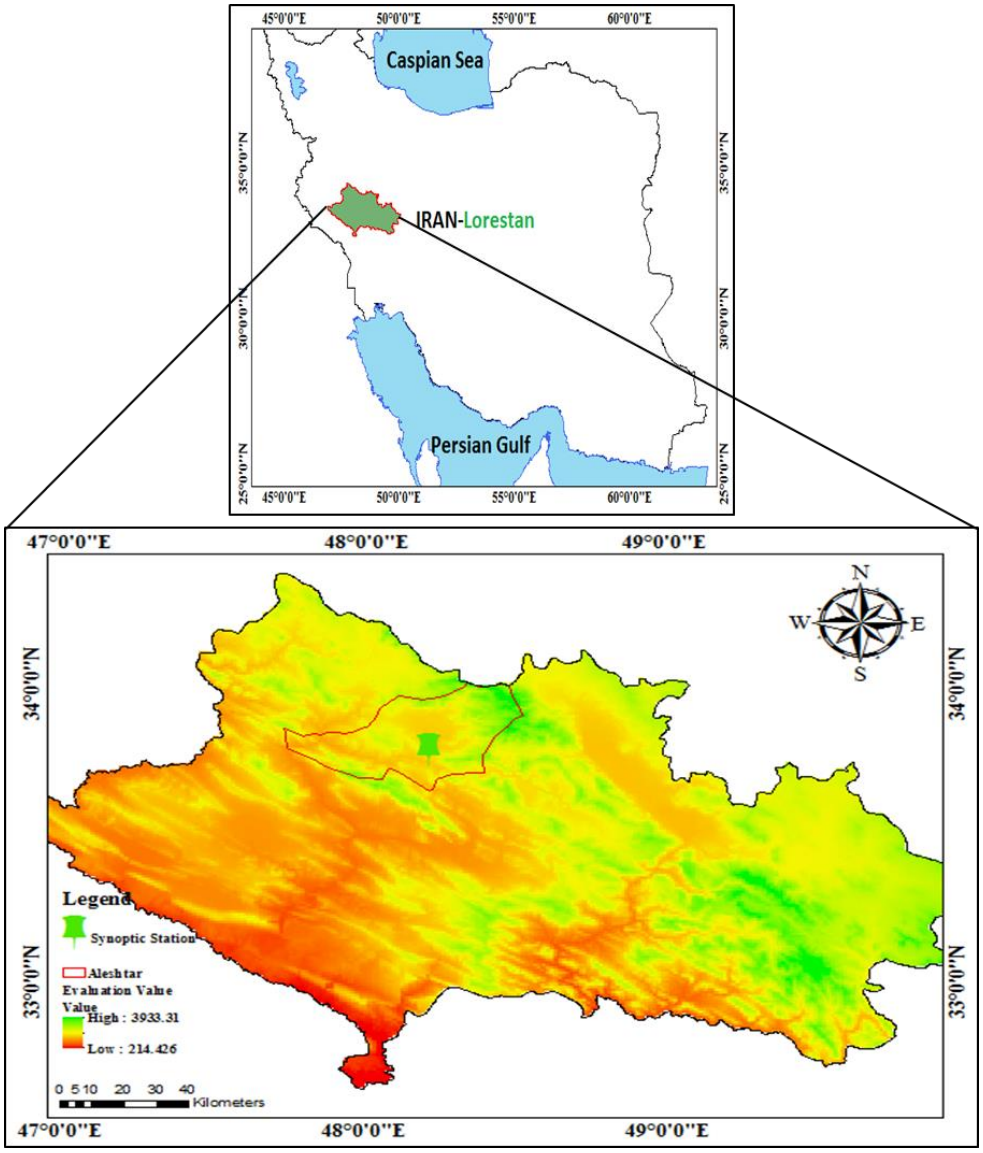

Figure 1. Study area

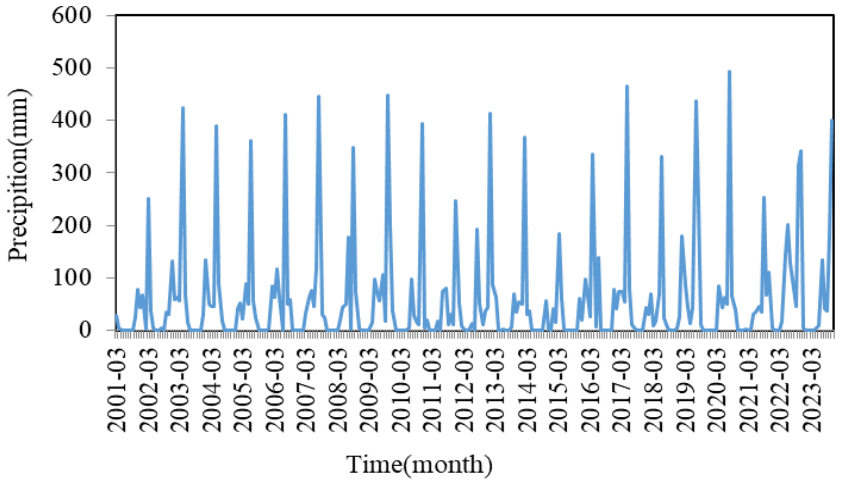

Figure 2. Precipitation status of the study area

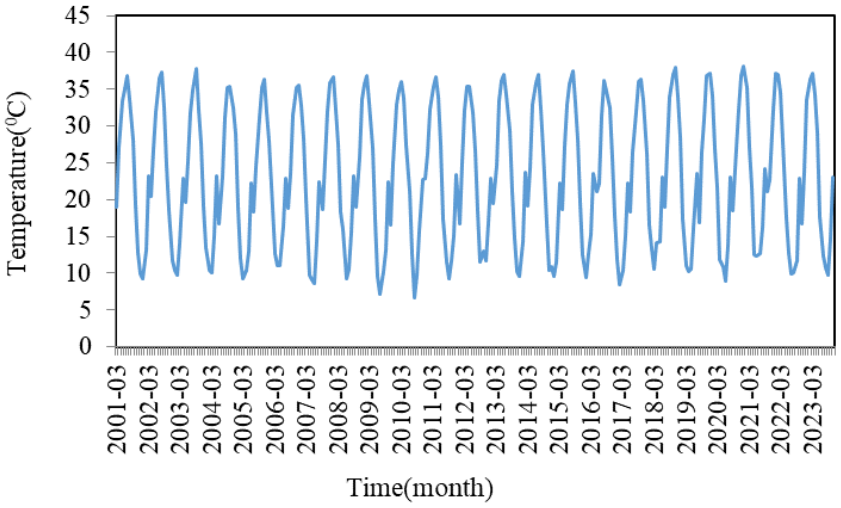

Figure 3. Temperature status of the study area

LARS-WG Downscaling Model

The LARS-WG model consists of three main parts: calibration, validation, and simulation of climatic conditions for future time decades. The model requires a file that specifies the climatic behavior of the study area during the base time period. To create this file, daily precipitation values, minimum and maximum temperatures, and sunshine hours are needed for a specific time period. The model can then use this file to simulate the conditions governing future periods. The first step in preparing the data for input into the LARS-WG model is calibration. In this step, approximately 75% of the historical period data, including precipitation, minimum temperature, and maximum temperature, is used. Then, the results from this step are compared with the remaining 25% of the historical period data to determine similarities. Analysis of the calibration process identifies the collected (observed) data to determine their characteristics and create a location-based cumulative probability distribution for various climatic variables. Based on the input data, the LARS-WG model produces the required files, including climatic parameters and seasonal distributions of wet and dry periods. During the simulation process, the number of years to be randomly determined controls the random components of climate generation (Irwin et al., 2012; Jahangir et al., 2022). The next step is to validate the results to ensure sufficient confidence in generating daily values of meteorological variables that have similar characteristics to the historical period data. In the validation stage, the remaining historical period data (25%) is used. The LARS-WG model is not a tool for predicting climatic or weather conditions, but rather for assessing the effects of climate change and weather conditions in future decades.

Input Data to the LARS-WG Model

In this study, data on precipitation, minimum temperature, maximum temperature, and sunshine hours were used in the base time period of 1997-2022.

SSP Scenarios

One of the limitations of the RCP scenario is the lack of a socio-economic narrative of expected demographic trends during the 21st century. Therefore, in this study, the Shared Socioeconomic Pathways (SSPs) scenarios were used. These scenarios describe narratives related to expected changes during the 21st century in relation to socio-economic dimensions, climate change, vulnerability, and the effectiveness of sustainable policies (Jones & O'Neill, 2016). Therefore, it is possible to analyze expected demographic changes during the 21st century. These scenarios are:

- **SSP1 (Sustainability):** The first scenario is based on a sustainable path in the 21st century, aiming to reduce inequality between countries and consumption with less resource intensity.

- **SSP2 (Middle of the Road):** This scenario differs from historical patterns of unequal growth among countries. In this scenario, international goals are pursued slowly.
- **SSP3 (Regional Rivalry):** In this scenario, nationalism emerges with policies focused on regional basins. Lack of international awareness of sustainable goals leads to environmental problems in various regions.
- **SSP4 (Inequality):** Inequality is increasing in various regions of the world. In the energy sector, renewable energy sources and fossil fuels have been developed.
- **SSP5 (Fossil-Fueled Development):** This scenario is based on a rapid increase in the global economy with increasing consumption of fossil fuels.

Evaluation of Data Produced by the Model Based on Observational Data

In order to evaluate the results of the LARS-WG model, the statistical parameters of the coefficient of determination (R2), Root Mean Square Error (RMSE), and Nash-Sutcliffe Efficiency (NSE) were used, the relationships of which are as follows:

$$R^2 = \frac{\sum_{i=1}^{n} X_i Y_i}{\sqrt{\sum_{i=1}^{n} X_i^2 \sum_{i=1}^{n} Y_i^2}} \quad (1)$$

$$RMSE = \sqrt{\frac{\sum_{i=1}^{n} (X_i - Y_i)^2}{n}} \quad (2)$$

$$NSE = 1 - \frac{\sum_{i=1} (X_i - Y_i)^2}{\sum_{i=1} (X_i - \overline{X})^2} \quad (3)$$

In the above relationships, Xi is the observed data, is the average of the observed data, and Yi is the modeled data.

Selection of the Most Compatible GCM Model with Observational Data

In this study, data from 15 new GCM models presented in the IPCC Sixth Assessment Report were downloaded (their information is provided in Table (1). Then, using the statistical parameters R2, NRMSE, and NSE, the data from the downloaded models were compared with the observational data. Finally, the CNRM-CM6-1 model was selected as the most compatible model with the observational data (Table 2). Subsequently, using the data from this model, the parameters of precipitation, minimum temperature, and maximum temperature were generated for future periods under the SSP scenarios.

Table 1. Information of GCM models introduced in the sixth IPCC report used in the present study

Row	Model	Country or Union	Atmospheric resolution	Integration period
1	ACCESS-ESM1	Australia	1.875° × 1.25°	1997-2022
2	BCC-CSM2-MR	China	~2.8° × 2.8°	1997-2022
3	CanESM5	Canada	~2.8° × 2.8°	1997-2022
4	CESM2	Italy	1.875° × ~1.9°	1997-2022
5	CMCC-ESM2	France	~1.4° × 1.4°	1997-2022
6	CNRM-CM6-1	France	~1.4° × 1.4°	1997-2022
7	GFDL-ESM4	USA	1.25° × 1°	1997-2022
8	GISS-E2-1-G	USA	2.5° × 2°	1997-2022
9	HadGEM3-GC31-LL	Russia	2° × 1.5°	1997-2022
10	INM-CM5-0	France	3.75° × ~1.9°	1997-2022
11	MIROC6	Japan	2.8125° × ~2.8°	1997-2022
12	MIROC-ES2L	Germany	1.875° × ~2°	1997-2022
13	MPI-ESM1-2-LR	Germany	1.125° × ~1.1°	1997-2022
14	MRI-ESM2-0	UK	1.875° × 1.25°	1997-2022
15	TaiESM1	UK	1.9° × 1.3°	1997-2022

Validation of the LARS-WG Model

Typically, two methods are used to validate the LARS-WG model. In the first method, the available data is divided into two categories. Then, climatic data is generated without defining any scenarios, and the validation process is performed with the data from the second category. In the second method, the performance of the *.tst file generated by the LARS-WG model can be evaluated using

statistical tests such as the F-test, t-student test, and Kolmogorov-Smirnov test. Also, the mean, standard deviation, and statistical distribution of the existing data are examined. The Kolmogorov-Smirnov (K-S) test is used to evaluate the compatibility of observational and generated data series in four cases: including the seasonal distribution of wet and dry series, the distribution of daily precipitation, the distribution of minimum temperature, and the distribution of maximum temperature. The t-student test is used to examine the significance of the difference between observational and generated time series for the parameters of mean monthly precipitation, mean monthly daily maximum temperature, and mean monthly daily minimum temperature. Finally, the F-test is used to examine the monthly variance of observed and generated precipitation data.

Table 2. Values of various statistical parameters in evaluating the correlation between historical data and GCM model data

Row	Model	Pr			T_{max}			T_{min}		
		R^2	NRMSE	NSE	R^2	NRMSE	NSE	R^2	NRMSE	NSE
1	ACCESS-ESM1	0.65	0.56	0.51	0.98	1.04	0.61	0.97	0.79	0.50
2	BCC-CSM2-MR	0.13	0.95	-0.44	0.68	0.72	0.51	0.72	1.64	-1.17
3	CanESM5	0.38	1.16	-1.13	0.71	0.75	0.38	0.82	1.77	-1.55
4	CESM2	0.16	1.23	-1.39	0.28	0.29	-1.86	0.21	2.53	-4.18
5	CMCC-ESM2	0.72	0.81	-0.04	0.71	0.75	0.71	0.96	0.70	0.60
6	**CNRM-CM6-1**	**0.90**	**0.87**	**0.68**	**0.99**	**1.05**	**0.64**	**0.97**	**0.68**	**0.63**
7	GFDL-ESM4	0.37	1.57	-2.89	0.67	0.72	0.70	0.96	0.62	0.69
8	GISS-E2-1-G	0.58	0.55	0.52	0.69	0.73	0.53	0.96	0.76	0.54
9	HadGEM3-GC31-LL	0.25	0.81	-0.03	0.43	0.46	0.50	0.03	1.01	0.17
10	INM-CM5-0	0.25	0.81	-0.03	0.43	0.46	0.50	0.03	1.01	0.17
11	MIROC6	0.82	0.61	0.41	0.61	0.65	0.57	0.96	0.58	0.73
12	MIROC-ES2L	0.44	0.88	-0.23	0.99	1.05	0.64	0.97	0.82	0.46
13	MPI-ESM1-2-LR	0.85	0.97	-0.48	1.00	1.06	0.84	0.97	0.79	0.50
14	MRI-ESM2-0	0.78	0.50	0.61	0.99	1.05	0.95	0.97	0.72	0.58
15	TaiESM1	0.13	0.90	-0.28	0.43	0.45	0.49	0.04	1.00	0.19

Table 3. Results of Kolomogrov-Smirnov, F-test and t-student tests between observational and generated data

	Minimum Temperature				Maximum Temperature				precipitation			
	K-S	t-student	F	P value	K-S	F	t-student	P value	K-S	F	t-student	P value
Jan	0.05	1.45	4.17	1.00	0.01	16.01	-0.35	1.00	0.07	1.17	0.30	1.00
Feb	0.05	0.44	5.27	1.00	0.05	19.41	0.13	1.00	0.13	1.19	-0.87	0.99
Mar	0.03	-1.95	4.26	1.00	0.05	19.05	-0.45	1.00	0.07	1.09	-0.29	1.00
Apr	0.05	-0.12	2.18	1.00	0.05	42.64	0.21	1.00	0.07	1.41	0.27	1.00
May	0.05	-0.66	7.16	1.00	0.03	26.56	-0.57	1.00	0.07	1.51	-1.76	1.00
Jun	0.05	-1.54	17.40	1.00	0.05	10.92	0.40	1.00	0.09	1.74	1.23	1.00
Jul	0.05	-0.20	9.28	1.00	0.11	12.56	0.77	1.00	0.61	6.75	-1.78	0.88
Aug	0.05	1.02	9.28	1.00	0.05	20.32	0.04	1.00	0.33	9.26	-1.78	0.80
Sep	0.03	-0.34	8.80	1.00	0.05	24.04	-0.39	1.00	0.61	5.42	-2.06	0.64
Oct	0.11	0.24	9.89	1.00	0.03	30.24	-0.24	1.00	0.06	3.65	-2.06	1.00
Nov	0.05	-0.01	6.63	1.00	0.05	17.94	-0.46	1.00	0.07	1.95	-1.76	1.00
Dec	0.03	-0.54	5.61	1.00	0.05	5.66	-0.63	1.00	0.06	1.04	-0.70	1.00

Results and Discussion

Model Validation in Simulating Precipitation and Temperature Variables

Figure 4 shows the average of the observed and simulated precipitation and average temperature data. As can be seen, the

difference between the observed data and the data simulated by the LARS-WG model is very small, which proves the high accuracy and ability of the LARS-WG model in downscaling precipitation and temperature parameters. Therefore, the mentioned data can be used to simulate precipitation and temperature variables in long-term future time intervals under the influence of climate change scenarios.

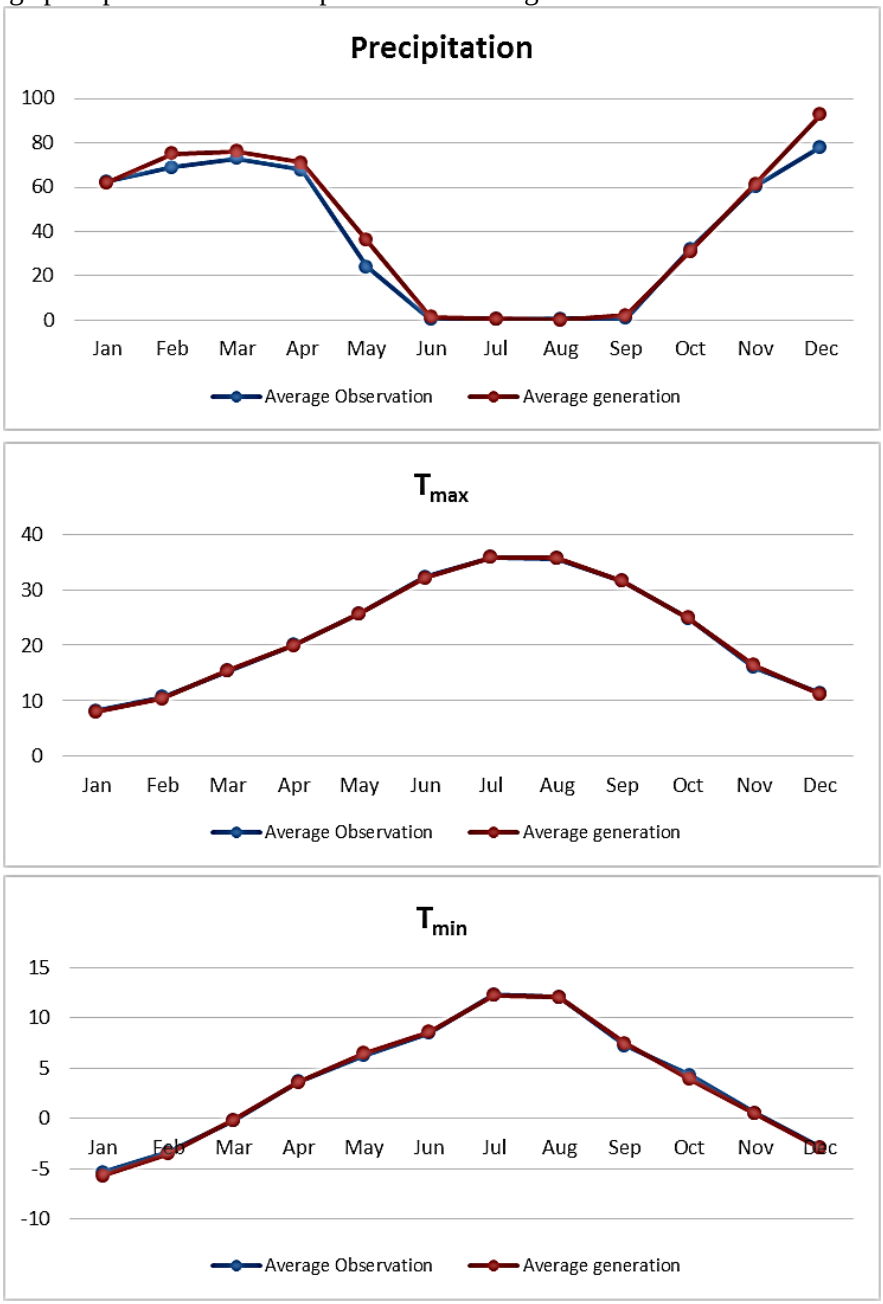

Figure 4. Comparison of observational and modeled values on a monthly scale

Monthly Results of Forecasting Meteorological Parameters in Future Scenarios

After validating the LARS-WG model, the minimum temperature, maximum temperature, and precipitation data at the Aleshtar station were predicted for the two time periods of 2031-2050 and 2051-2070 AD for the SSP126, SSP245, and SSP585 scenarios using the data from the CNRM-CM6-1 model. The monthly results of forecasting the mentioned parameters are

shown in Figure 5. According to this figure, it is observed that monthly precipitation in future periods compared to the base period has an increasing trend in the months of January to April and October to December, with the highest increase in the months of February and December.

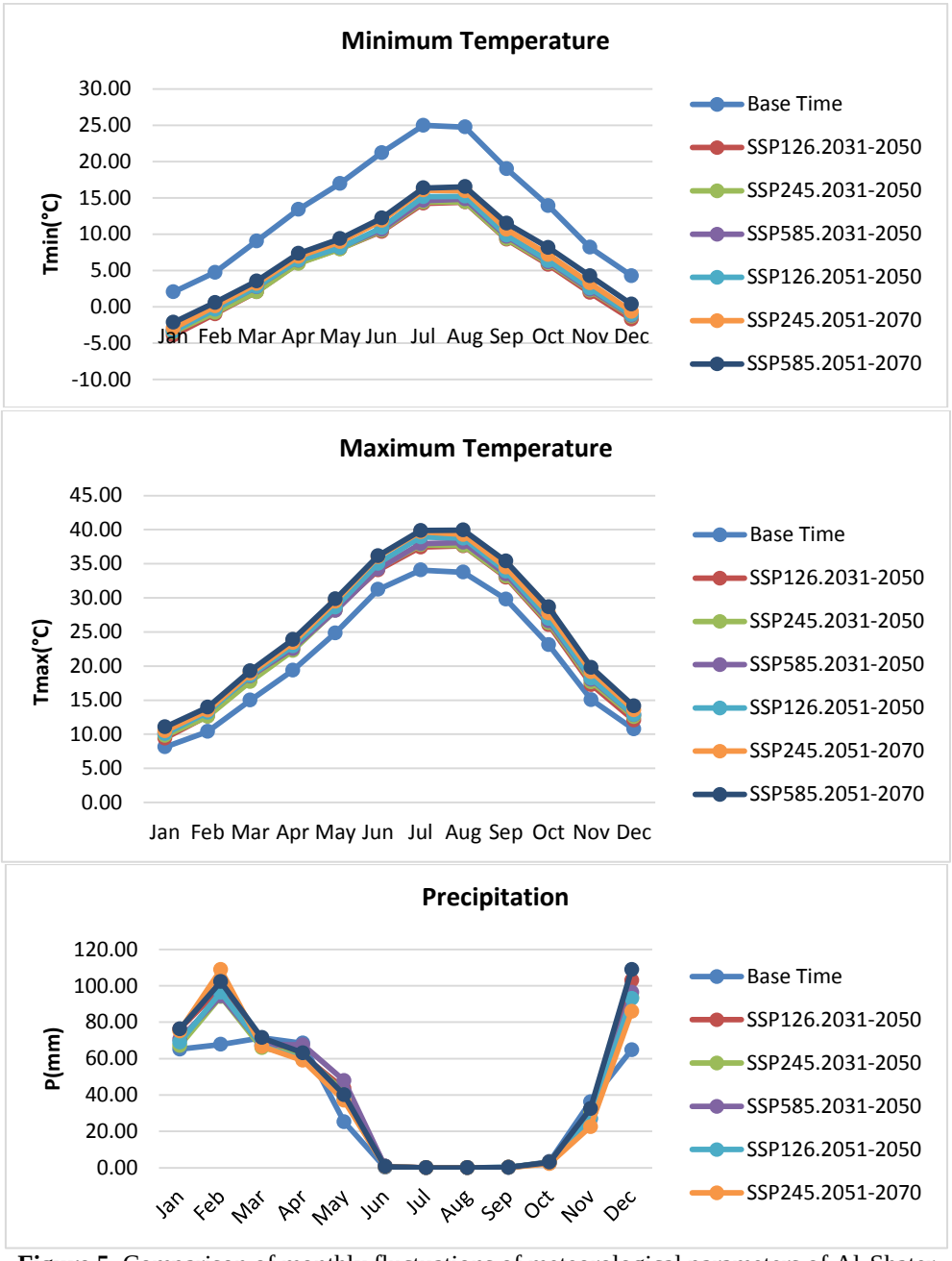

Figure 5. Comparison of monthly fluctuations of meteorological parameters of Al-Shater station in future time periods compared to the base period

The minimum temperature in the future period compared to the base period has a decreasing trend. The lowest temperature decrease is observed in the SSP126 scenario, and the highest decrease is observed in the SSP585 scenario. Regarding precipitation,

the amount of precipitation in the future period compared to the base period shows an increasing trend in the SSP126 scenario and a decreasing trend in the SSP585 scenario. The amount of changes in the minimum temperature, maximum temperature, and precipitation parameters for the two future periods compared to the base period are shown in Tables 4 to 6. In general, in the SSP126 scenario, compared to the base period, the minimum temperature and precipitation decrease, and the maximum temperature increases. The highest increase in precipitation is estimated in the month of June for the SSP126 scenario, and the lowest increase is estimated in the month of November for the SSP585 scenario. The lowest minimum temperature is also predicted in the SSP126 scenario, and the highest minimum temperature is predicted in the SSP585 scenario. Regarding the maximum temperature, the lowest and highest temperature fluctuations were predicted in the SSP126 and SSP585 scenarios, respectively.

Table 4. Precipitation fluctuations in future periods compared to the base period in climate scenarios (percentage)

	2031-2050			2051-2070		
	SSP126	**SSP245**	**SSP585**	**SSP126**	**SSP245**	**SSP585**
Jan	14.42	2.92	7.64	5.57	13.28	14.50
Feb	31.52	27.95	28.13	29.67	37.71	33.70
Mar	-6.67	-8.39	-5.59	-6.50	-7.21	0.08
Apr	-10.79	-10.25	-1.31	-15.06	-16.08	-8.44
May	41.99	39.09	47.19	33.47	31.62	36.96
Jun	85.57	83.63	86.70	81.27	80.61	83.64
Jul	29.55	21.81	37.58	23.49	12.15	29.55
Aug	-3.02	-10.23	3.31	3.31	-7.02	3.31
Sep	84.26	82.26	84.39	84.93	84.75	84.85
Oct	-11.39	-14.09	-31.98	-29.03	-47.27	-11.91
Nov	-18.11	-17.99	-35.82	-33.20	-60.47	-11.62
Dec	37.05	30.71	32.70	30.26	24.48	40.46

Table 5. Minimum temperature fluctuations in future periods compared to the base period in climate scenarios (percentage)

	2031-2050			2051-2070		
	SSP126	**SSP245**	**SSP585**	**SSP126**	**SSP245**	**SSP585**
Jan	-292.83	-270.61	-262.75	-265.16	-245.23	-205.65
Feb	-121.10	-117.01	-106.42	-107.61	-98.01	-87.76
Mar	-77.28	-77.33	-69.84	-69.40	-64.77	-60.85
Apr	-55.11	-55.60	-52.32	-52.25	-48.36	-45.26
May	-52.85	-53.15	-51.92	-52.07	-47.32	-44.76
Jun	-51.09	-50.39	-49.88	-48.66	-44.00	-42.47
Jul	-42.98	-42.24	-41.50	-39.33	-35.74	-34.52
Aug	-41.76	-41.59	-40.05	-38.48	-35.48	-33.17
Sep	-51.22	-50.71	-49.08	-48.13	-43.94	-39.45
Oct	-58.26	-56.76	-55.68	-54.44	-48.33	-41.41
Nov	-76.10	-72.41	-70.91	-68.60	-60.03	-47.82
Dec	-140.61	-131.07	-128.19	-125.86	-115.38	-91.97

Table 6. Maximum temperature fluctuations in future periods compared to the base period in climate scenarios (percentage)

	2031-2050			2051-2070		
	SSP126	**SSP245**	**SSP585**	**SSP126**	**SSP245**	**SSP585**
Jan	15.85	20.62	25.37	23.83	28.99	36.14
Feb	21.94	21.45	29.47	27.30	29.99	34.37
Mar	19.61	18.30	23.48	24.31	26.14	28.72
Apr	16.17	14.94	16.44	18.40	20.95	23.23
May	13.97	13.33	13.10	15.15	18.55	20.03
Jun	9.11	9.88	9.64	12.22	15.35	15.82
Jul	9.90	10.88	11.33	14.24	16.49	17.04

Aug	11.42	11.60	12.94	14.73	16.31	18.25
Sep	10.71	11.26	12.33	13.69	15.65	18.66
Oct	12.69	13.85	15.07	16.51	20.02	23.97
Nov	14.71	17.39	19.78	20.89	27.30	31.49
Dec	12.17	16.77	19.44	19.88	26.29	31.53

Figure 6 displays monthly box plots comparing the examined climate scenarios. The box plots reveal distinct differences between various climate scenarios. In the SSP1-2.6 scenario, representing a stable, low-carbon pathway, the data distribution is more concentrated with a smaller interquartile range (IQR), indicating less variability in precipitation patterns. In contrast, the SSP5-8.5 scenario, considered a high-carbon and more pessimistic pathway, not only shows a lower median but also exhibits a wider IQR and more outliers. These characteristics suggest more intense climate fluctuations and an increased likelihood of extreme events such as heavy rainfall or prolonged drought periods under this scenario.

From a statistical perspective, non-parametric tests like the Mann-Whitney U test confirm significant differences between the scenarios. Specifically, comparing the extreme scenarios (SSP1-2.6 versus SSP5-8.5) reveals not only a decrease in average precipitation but also a noticeable increase in climate system instability. These findings are crucial for water resource management and environmental planning, highlighting the urgent need to reduce greenhouse gas emissions. The results clearly demonstrate that choosing low-carbon development pathways can lead to greater climate system stability and reduced risks associated with extreme events.

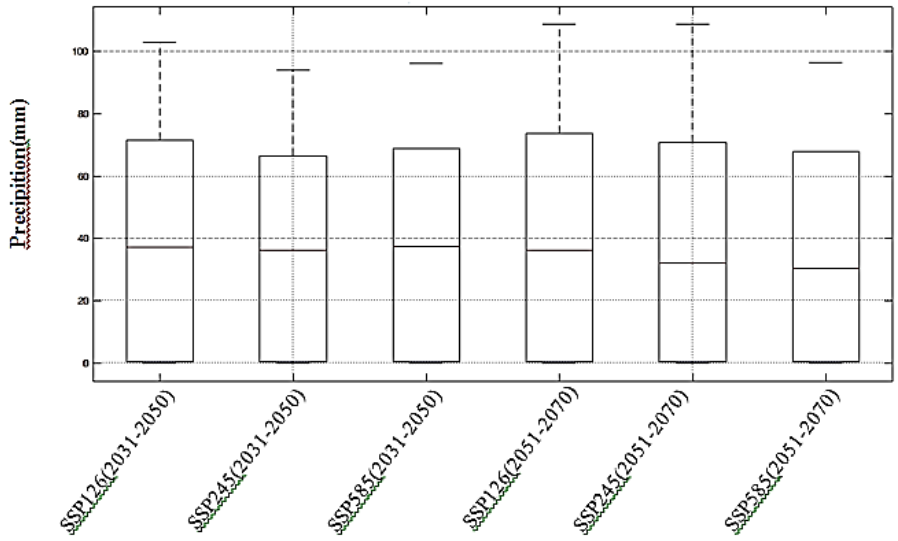

Figure 6. Combined box plot of the scenarios studied

Seasonal Results of Forecasting Meteorological Parameters in Future Scenarios

The seasonal results of forecasting the minimum temperature, maximum temperature, and precipitation parameters of the Aleshtar station in future periods under the SSP scenarios are presented in Figure 7. It is observed that the highest seasonal minimum temperature is estimated in the summer season under the SSP585 scenario, and the lowest minimum temperature is estimated in the winter season under the SSP126 scenario. The highest maximum temperature is also estimated in the summer season under the SSP585 scenario, and the lowest maximum temperature is estimated in the winter season under the SSP126 scenario. In addition, the highest precipitation is estimated in the spring season under the

SSP126 scenario, and the lowest precipitation is estimated in the summer season under the SSP585 scenario.

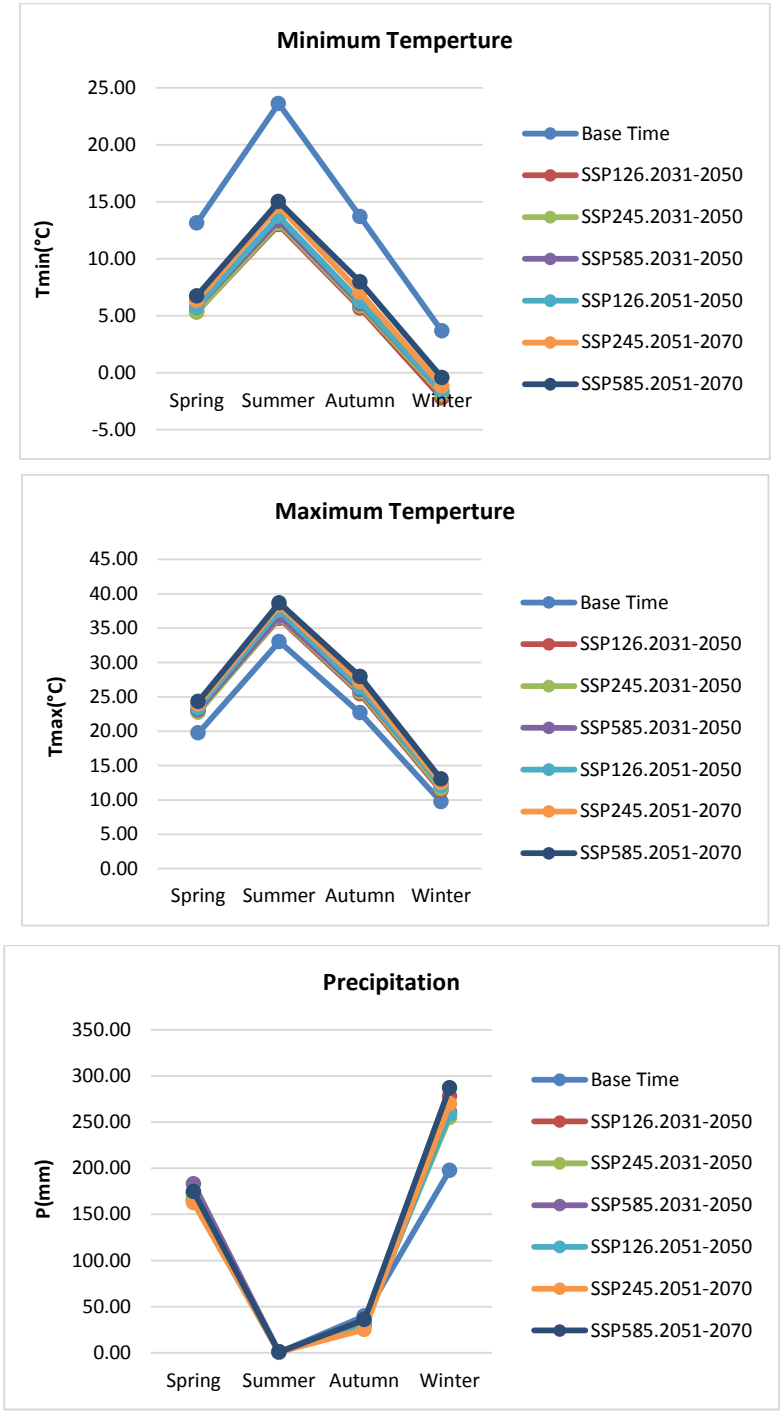

Figure 7. Seasonal results of modeling meteorological parameters in future periods under SSP scenarios

Conclusion

This study employed the CanESM5.0 climate prediction model from the Sixth Assessment Report (CMIP6) to investigate the impacts of climate change on temperature and precipitation variables recorded at the AleshtarSynoptic Station in Lorestan Province, Iran. Using baseline data from 1997-2022, the research projected future climate conditions under three emission scenarios:

the optimistic SSP1-2.6, intermediate SSP2-4.5, and pessimistic SSP5-8.5, examining two future 25-year periods: near-term (2031-2050) and mid-term (2051-2070). The model performance analysis revealed that while CanESM5.0 accurately simulates maximum and minimum temperature parameters, it demonstrates higher errors in precipitation simulation. Key findings include: Under the SSP1-2.6 scenario, minimum temperature and precipitation show decreasing trends compared to the baseline period, while maximum temperature increases. Simulated temperatures under SSP1-2.6 exhibit an increasing trend during June to October in both future periods. Precipitation demonstrates an increasing trend from January to June and October to December in future periods. Seasonal analysis indicates rising temperatures in spring and summer, with increased precipitation in autumn and winter. These findings provide reliable scientific evidence to support climate change adaptation and mitigation strategies, serving as a valuable resource for policymakers, organizations, and the scientific community in making informed decisions to address climate change impacts.

References

Acar, Z., Gönençgil, B. 2022. Investigation of extreme precipitation indices in Turkey. Theoretical and Applied Climatology. 148, 679–691.

Adhikari, U., Nejadhashemi, A.P., Woznicki, S.A. 2015. 2018. Climate change and eastern Africa: a review of impact on major crops. Food and Energy Security. 4 (2), 110–132.

Amirabadizadeh, M., Ghazali, A.H., Huang, Y.F., Wayayok, A. 2016. Downscaling daily precipitation and temperatures over the Langat River Basin in Malaysia: A comparison of two statistical downscaling approaches. International Journal of Water Resources and Environmental Engineering 8 (December), 120–136.

Basile, S.M.L., Tognetti, J.A., Gandini, M. l., Rogers, W. l. 2022. Climate change in the temperature and precipitation at two contrasting sites of the Argentinean wheat region. Theoretical and Applied Climatology . 148, 237–254.

Ferreira, R.N,, Nissenbaum, M.R., Rickenbach, T.H.M. 2018. Climate change effects on summertime precipitation organization in the Southeast United StatesAtmospheric Research. 214, 348–363.

Gebrechorkos, S.H., Hülsmann, S., Bernhofer, C. 2019. Statistically downscaled climate dataset for East Africa. Scientific data. 6, 31-42.

Heydari, S.H., Hosseini, S.A., Heydari, A.A. 2020. Investigating the effects of climate change on stream flows of Urmia Lake basin in Iran. Modeling Earth Systems and Environment. 1, 329–339.

IPCC. 2021. Climate Change 2021: The Physical Science Basis. A special report of Working group, I contribution to the IPCC Sixth Assessment Report (AR6-WG1).

Irwin, S.E., et al., 2012. Assessment of Climatic Vulnerability in the Upper Thames River Basin: Downscaling with LARS-WG. Water Resources Research Report. The University of Western Ontario, Department of Civil and Environmental Engineering.

Jahangir, M.H., Haghighi. P., Danehkar. S.h. 2022. Downscaling climate parameters in Fars province, using models of the fifth report and RCP scenarios. Ecological Informatics. 68(4), 101-122.

Javaherian, M., Ebrahimi,, H., Aminnejad, B. 2020. Prediction of changes in climatic parameters using CanESM2 model based on Rcp scenarios (case study): Lar dam basin" Ain Shams Engineering Journal. 12,445–454.

Jiang, L., O'Neill, B.C. 2017. Global urbanization projections for the shared socioeconomic pathways. Global Environmental Change. 42 , 193–199.

Jones, B., Neill, B.C.O. 2016. Spatially explicit global population scenarios consistent with the Shared Socioeconomic Pathways. Environmental Research Letters. 11 , 1–10.

Majdai. F., Hosseini. S. A., Karbalaee. A., Kaseri. M., Marjanian. M. 2022. Future projection of precipitation and temperature changes in the Middle East and North Africa (MENA) region based on CMIP6. Theoretical and Applied Climatology .147,1249–1262.

Mwabumba, M., Yadav. B.K., Mwemezi. J.R., Larbi. I., Dotse. S.Q., Limantol. A.M., Sarpong. S., Kewawuvi. D. 2022. Rainfall and temperature changes under different climate scenarios at the watersheds surrounding the Ngorongoro Conservation Area in Tanzania. Environmental Challenges. 7, 56-72.

Qin, J., Su, B., Tao, H., Wang, Y., Huang, j., Jiang, T. 2021. Projection of temperature and precipitation under SSPs-RCPs Scenarios over northwest China. Frontiers in Earth Science. 15, 23–37.

Saraf, V.R., Regulwar, D.G. 2016. Assessment of Climate Change for Precipita- tion and Temperature Using Statistical Downscaling Methods in Upper Go- davari River Basin. India. Journal of Water Resource and Protection. 8, 31–45.

Try, S., Tanaka. S., Tanaka. K., Sayama. T., Khujanazarov. T., Oeurng. C. 2022. Comparison of CMIP5 and CMIP6 GCM performance for flood projections in the Mekong River Basin. Journal of Hydrology: Regional Studies. 40, 101-114.

Weijing, L., Jinging, Z., Yanling, S., Jingpeng, L., Yu, L., Yuyang, S., Jingxin, L. 2015. Changes in spatio-temporal distribution of drought/flood disaster in southern china under global climate warming. Meteorol Mon (in Chinese). 41, 261–271.

Yue, Y., Yan, D., Yue, Q., Ji, G., Wang, Z. 2021. Future changes in precipitation and temperature over the Yangtze River Basin in China based on CMIP6 GCMs, Atmospheric Research. 264, 761-782.

Zhang, H., Zhao. J., Huang. B., Zang. N., Yang. J., Feng. G. 2022. The variabilities of convective precipitation and large‐scale precipitation in southern China for the period 1980–2020. Journal of Theoretical and Applied Climatology. 24, 221-232.

Zhang, R.H. 2015. Natural and human-induced changes in summer climate over the East Asian monsoon region in the last half century: a review. Advances in Climate Change Research. 6,131–140.